BIOCHEMISTRY
including biophysical chemistry & molecular biology

Article

pubs.acs.org/biochemistry

Methylated N^{ω}-Hydroxy-L-arginine Analogues as Mechanistic Probes for the Second Step of the Nitric Oxide Synthase-Catalyzed Reaction

Kristin Jansen Labby,[†] Huiying Li,[‡] Linda J. Roman,[§] Pavel Martásek,[§,∥] Thomas L. Poulos,*[,‡] and Richard B. Silverman*[,†]

[†]Department of Chemistry, Department of Molecular Biosciences, Chemistry of Life Processes Institute, and Center for Molecular Innovation and Drug Discovery, Northwestern University, 2145 Sheridan Road, Evanston, Illinois 60208-3113, United States

[‡]Departments of Molecular Biology and Biochemistry, Chemistry, and Pharmaceutical Sciences, University of California, Irvine, California 92697-3900, United States

[§]Department of Biochemistry, University of Texas Health Science Center, San Antonio, Texas 78384-7760, United States

[∥]Department of Pediatrics, First School of Medicine, Charles University, Prague, Czech Republic

Supporting Information

ABSTRACT: Nitric oxide synthase (NOS) catalyzes the conversion of L-arginine to L-citrulline through the intermediate N^{ω}-hydroxy-L-arginine (NHA), producing nitric oxide, an important mammalian signaling molecule. Several disease states are associated with improper regulation of nitric oxide production, making NOS a therapeutic target. The first step of the NOS reaction has been well-characterized and is presumed to proceed through a compound I heme species, analogous to the cytochrome P450 mechanism. The second step, however, is enzymatically unprecedented and is thought to occur via a ferric peroxo heme species. To gain insight into the details of this unique second step, we report here the synthesis of NHA analogues bearing guanidinium methyl or ethyl substitutions and their investigation as either inhibitors of or alternate substrates for NOS. Radiolabeling studies reveal that N^{ω}-methoxy-L-arginine, an alternative NOS substrate, produces citrulline, nitric oxide, and methanol. On the basis of these results, we propose a mechanism for the second step of NOS catalysis in which a methylated nitric oxide species is released and is further metabolized by NOS. Crystal structures of our NHA analogues bound to nNOS have been determined, revealing the presence of an active site water molecule only in the presence of singly methylated analogues. Bulkier analogues displace this active site water molecule; a different mechanism is proposed in the absence of the water molecule. Our results provide new insights into the steric and stereochemical tolerance of the NOS active site and substrate capabilities of NOS.

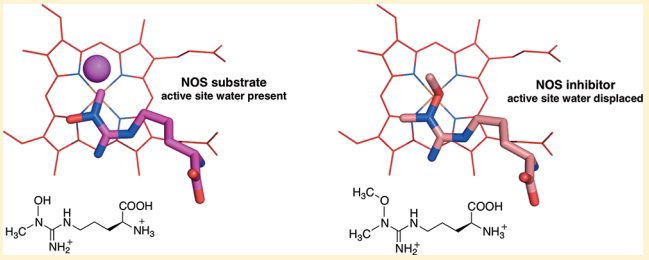

Nitric oxide synthases (NOSs) catalyze the oxygenation of L-arginine to L-citrulline and nitric oxide (NO) using molecular oxygen (O_2) and NADPH (Scheme 1). NO is an important signaling molecule with a wide range of biological functions.[1−3] There are three mammalian NOS isoforms. As products of distinct genes, they maintain highly conserved active sites across all three isoforms and other species. Two are constitutive isoforms, neuronal NOS (nNOS) and endothelial NOS (eNOS), which are involved in neuronal signaling and vascular regulation, respectively.[4,5] Inducible NOS (iNOS) is expressed in macrophage cells in response to the invasion of pathogens.[3] Misregulation of NO production has been implicated in various disease states,[1−3] and therefore, NOSs are sought-after therapeutic targets. A better understanding of the NOS mechanism will aid in the design of novel NOS inhibitors.

NOSs are homodimeric enzymes with a reductase domain that binds NADPH, FAD, and FMN and an oxygenase domain that contains heme and binds L-arginine and (6*R*)-5,6,7,8-tetrahydrobiopterin (H_4B). The mechanism catalyzed by NOS occurs in two distinct steps (Scheme 1). In the first step, L-arginine is monooxygenated to N^{ω}-hydroxy-L-arginine (NHA). This is proposed to occur through an oxygen rebound mechanism via the compound I (CpdI, $Fe^{IV\bullet+}$=O) heme species, analogous to cytochrome P450 chemistry (Scheme 2).[6] H_4B provides the second electron required for oxygen activation.[7,8] In the second step, NOS converts NHA to citrulline and NO, which requires only one electron. This step is thought to proceed through a ferric peroxo species.[9,10] Early mechanistic proposals included the nucleophilic addition of the ferric peroxide heme species (Fe^{III}−OO^-) to the guanidino carbon of NHA.[11−14] Recent electron paramagnetic resonance (EPR) and electron-nuclear double resonance (ENDOR) cryoreduction−annealing experiments provide evidence that

Received: November 21, 2012
Revised: April 14, 2013
Published: April 15, 2013

Scheme 1. Reaction Catalyzed by NOS

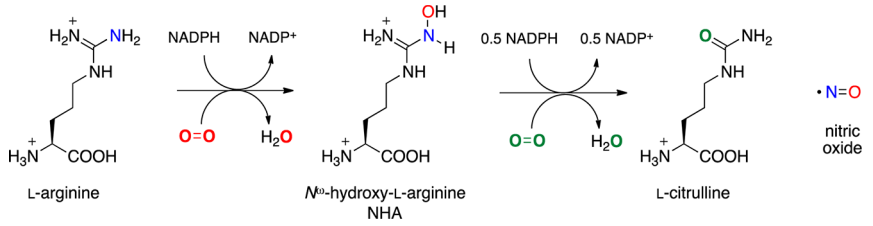

Scheme 2. Proposed NOS Mechanisms for Steps 1 and 2

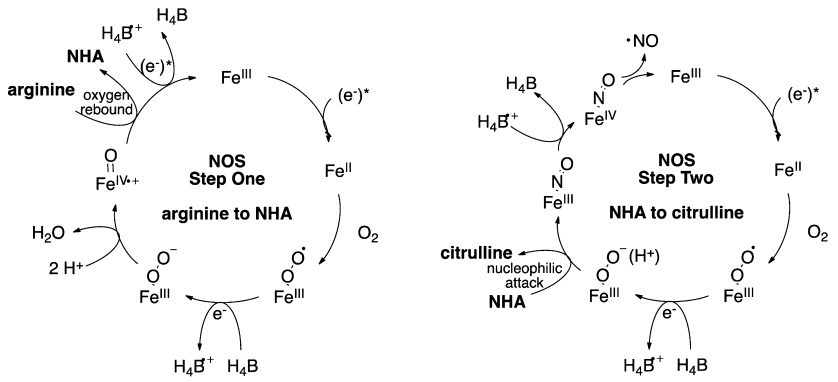

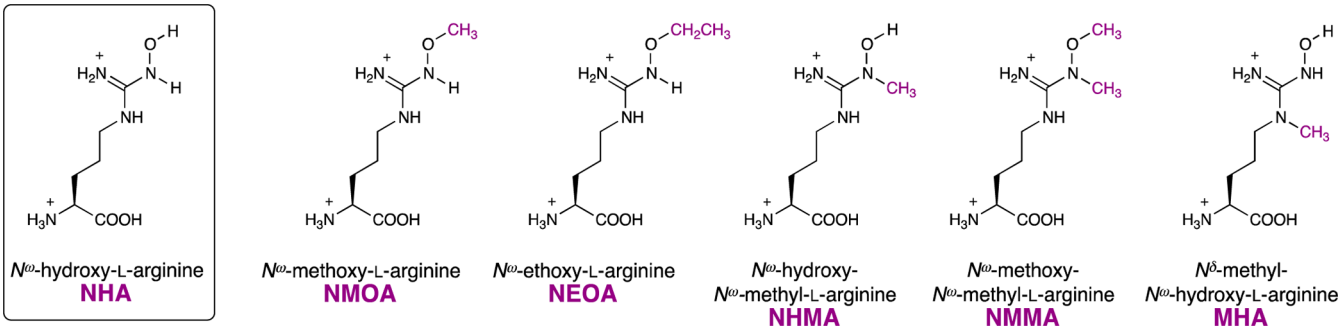

Figure 1. NHA substrate analogues.

an active species is ferric hydroperoxide ($Fe^{III}OOH$), and in this case, the mechanism could involve a nucleophilic attack of the hydroperoxide on the guanidinium oxime.[15] The source of the proton that forms $Fe^{III}OOH$ is unknown, but it is thought to be either an active site water molecule or the substrate itself.[14] The tetrahedral intermediate formed from addition of a ferric peroxo will then collapse, yielding citrulline and nitric oxide. In this step, H_4B also serves as a donor of the electron required for oxygen activation. It further acts as an electron acceptor when it is re-reduced either by the tetrahedral intermediate before collapse or by product NO^-, because overall this reaction is only a one-electron oxidation.[7] Substrate identity and, perhaps more importantly, its pK_a (arginine pK_a = 12.5; NHA pK_a = 8.5)[16] are thought to dictate the formation of these different active heme species in steps 1 and 2.

Although many experiments have been reported, details of the NOS mechanism remain elusive. During NOS turnover, the precise role of H_4B and, when it is implicated, the true identity of the active heme species and the source of protons (and how many are required) are still controversial.[17,18] An active site water molecule has been thought to play an important role in proton donation, either as a single proton donor or as a shuttle sequestering protons from the bulk solvent to the reaction site.[15,16,19] NOS crystal structures of various isoforms show a conserved, specifically oriented water molecule as part of a hydrogen bonding network that includes the substrate, active site residues, and the diatomic heme ligand (O_2 for catalysis, but NO and CO are used to form stable crystal structures).[13,20] A second hypothesis is that the substrate itself acts as a proton donor; ENDOR and X-ray experiments show that NHA is most likely protonated in the active site.[21] Furthermore, Davydov and Hoffman's cryoreduction EPR experiments showed that $Fe^{III}OOH$ formation is not pH-dependent, suggesting the proton is taken directly from NHA, not bulk solvent.[15]

The first NOS half-reaction closely resembles well-known cytochrome P450 hydroxylation chemistry, but the second-half reaction, the oxidation of an N^{ω}-hydroxyguanidine to a urea and NO, is enzymatically unprecedented. It is therefore poorly understood. Previously, we demonstrated that direct abstraction of a hydrogen atom from the O−H bond of NHA is not necessary for substrate turnover; N^{ω}-*tert*-butyloxy-L-arginine (tBOA) and N^{ω}-(3-methyl-2-butenyl)oxy-L-arginine are nitric oxide- and citrulline-producing NOS substrates.[22] To further probe the second step of the mechanism of NOS, we have synthesized and investigated a series of methylated (or ethylated) NHA analogues (Figure 1).

dx.doi.org/10.1021/bi301571v | *Biochemistry* 2013, 52, 3062−3073

N^{ω}-Methoxy-L-arginine (NMOA) has been previously synthesized[23,24] and has been explored as a prodrug inhibitor of arginase[25] but has not been examined as a NOS substrate. N^{ω}-Methyl-L-arginine (NMA) functions as an inactivator (k_{inact} = 0.07 min^{-1}; K_i = 2.7 μM), a competitive inhibitor (K_i = 200 nM), and a slow, alternative substrate for NOS.[26] NOS converts NMA into N^{ω}-hydroxy-N^{ω}-methyl-L-arginine (NHMA), which is subsequently converted into citrulline, NO, and formaldehyde.[26] As substrates, NMA and NHMA both cause significant uncoupling of NADPH oxidation.[26] N^{δ}-Methyl-L-arginine (δMA) can be converted by NOS to N^{δ}-methyl-N^{ω}-hydroxy-L-arginine (MHA), but no further.[27,28] δMA binds weakly to the NOS active site with a K_i of 1.4 mM.[27] N^{ω}-Methoxy-N^{ω}-methyl-L-arginine (NMMA) and N^{ω}-ethoxy-L-arginine (NEOA) have not been previously reported. We previously evaluated tBOA as a NOS substrate,[22] and here we re-examine a cocrystal structure of this compound bound in the nNOS active site. In this report, we present the synthesis, enzymatic evaluation, cocrystal structures, and novel mechanistic insights with respect to these five substrate analogues (Figure 1) as they relate to the second step of the NOS catalytic mechanism (Scheme 2).

MATERIALS AND METHODS

General Methods. All chemicals, unless otherwise noted, were obtained from Sigma-Aldrich and used without further purification. Michaelis–Menten kinetics and nonlinear regressions were plotted and analyzed using GraphPad Prism version 5.0c. Complete procedures for the syntheses, as well as the characterization of NMOA, NEOA, NEOA, NHMA, NMMA, MHA, and [^{14}C]NMOA, can be found in the Supporting Information.

Measuring NO Production. Murine iNOS[29] and rat nNOS[30] were expressed and purified from *Escherichia coli* as previously described. NO production was monitored using the hemoglobin capture assay at 22 °C.[31] In addition to various final concentrations of the analogue being evaluated, assay mixtures contained 100 μM NADPH, 3 μM hemoglobin-A0 (Sigma catalog no. H0267), and 10 μM H_4B, in 100 mM HEPES with 10% glycerol (pH 7.5). For nNOS assays, 1 mM $CaCl_2$ and 300 units/mL CaM were added. For the determination of K_i, assays contained 10 μM L-arginine. Assays were initiated via the addition of enzyme (final concentration of approximately 100 nM), and methemoglobin formation was monitored for 1 min at 401 nm using a Shimadzu UV-1800 spectrophotometer. K_m and k_{cat} values were determined from nonlinear regressions (Michaelis–Menten). For K_i determinations, IC_{50} values were first calculated using nonlinear regressions (dose–response inhibition, four-parameter variable slope). Subsequent K_i values were determined using the Cheng–Prushoff relationship: $K_i = IC_{50}/(1 + [S]/K_m)$ (a K_m of 8.3 μM was used for murine iNOS).[32]

When noted, NO production was also measured with the Greiss reagent[31] using the nitrite/nitrate colormetric assay kit from Cayman Chemical (catalog no. 760871). Enzyme incubations contained various concentrations of the compound being evaluated, 100 nM iNOS, 100 μM NADPH, and 10 μM H_4B, in 100 mM HEPES with 10% glycerol (pH 7.5). Lactate dehydrogenase was added to the reaction mixtures to oxidize excess NADPH, and then Griess reagents were added to report nitrate. The absorbance was measured at 540 nm using a Synergy H1 Biotek plate reader.

Determination of the Spectral Binding Constant, K_s. Binding affinities for iNOS were determined using the previously described ferric difference spectral binding assay.[33] Because all compounds were type I, a type II coordinating compound, imidazole, was used to initially coordinate to the heme. The K_s value was then determined from displacement of the imidazole. To a 500 μL quartz cuvette were added 5 μM iNOS, 10 μM H_4B, and 100 mM HEPES (pH 7.5) until the total volume reached 200 μL. This cuvette was scanned against a blank containing 100 mM HEPES with 10 μM H_4B. Spectra were recorded from 380 to 500 nm. To determine the binding affinity of imidazole, spectra were taken after the addition of aliquots of the imidazole (final concentration of 0.5–1 mM). To assay NHA analogues, 300 μM imidazole was used, aliquots of the analogue being examined (final concentration of 0.1–1 mM) were added, and spectra were obtained for each. The total volumes added were kept below 10 μL (5%) to avoid dilution effects. Michaelis–Menten curves were determined for the imidazole as well as for each inhibitor by plotting concentration versus absorbance difference (local maximum − local minimum). Then Hanes–Wolff plots were used to determine the K_s for imidazole and the apparent K_s for the NHA analogues.[34] The K_s for imidazole with iNOS was found to be 120–150 μM over multiple experiments; K_s values of analogues were determined using the following equation:

$$\text{apparent } K_s = \text{actual } K_s(1 + [\text{imidazole}]/K_{s\,\text{imidazole}})$$

NDA Derivatization and High-Performance Liquid Chromatography (HPLC) Separation. NDA derivatization reaction mixtures contained 25 μL of amino acid standard or sample, 25 μL of 30 mM NaCN in 100 mM $NaB(OH)_3$ buffer (pH 10), and 15 μL of 10 mM NDA in methanol. NDA reactions achieve completion nearly immediately, so all reactions were analyzed after 10 min. Phenylalanine was used as an internal standard to track complete derivatization and ensure complete injection. Reactions were analyzed by reversed-phase HPLC (10 μL injection) using an Econosil C18 column with 80% 5 mM sodium acetate (pH 6.0) and 20% MeOH as solvent A and 100% acetonitrile as solvent B. A gradient from 25 to 75% B was run over 30 min at a rate of 0.75 mL/min. Under these conditions, NDA-derivatized amino acids had the following retention times: citrulline, 4.2 min; phenylalanine, 9.4 min; NHA, 10.5 min; NMOA, 11.7 min; NHMA, 11.2 min; NMMA, 12.8 min. An NDA–citrulline standard curve (R^2 = 0.995) was linear from 100 μM to 1 mM.

Measuring Substrate Uncoupling. iNOS–substrate enzyme rections [300 μL total volume in quartz cuvettes, containing 100 μM NADPH, 10 μL of H_4B, 100 nM iNOS, 3 μM hemoglobin-A0, and 100 mM HEPES (pH 7.5)] were dually monitored at 401 and 340 nm for 1 min. Substrates were evaluated at the following final concentrations: 20 μM arginine, 20 μM NHA, 100 μM NMOA, and 100 μM NHMA. Reactions were initiated by the addition of iNOS. The following extinction coefficients were used: ε_{MetHb} = 38000 M^{-1} cm^{-1}, and ε_{NADPH} = 6.22 mM^{-1} cm^{-1}.[35]

DNPH Derivatization Reactions. DNPH derivatization reaction mixtures were set up by combining 20 μL of aldehyde standard or sample with 10 μL of 20 mM DNPH in 0.4 M H_2SO_4 in 10% H_2O and 90% acetonitrile. DNPH derivatization reactions proceed quickly to completion, so all reaction mixtures were injected after 10 min. All DNPH-derivatized reaction mixtures were separated by reverse-phase HPLC (10 μL injection) under the following conditions. A Phenomonex

dx.doi.org/10.1021/bi301571v | Biochemistry 2013, 52, 3062–3073

Table 1. Crystallographic Data Collection and Refinement Statistics[a]

	nNOS−NMOA	nNOS−NEOA	nNOS−NHMA	nNOS−NMMA	nNOS−MHA	nNOS−tBOA
			Data Collection			
PDB entry	4FVW	4FVX	4FVY	4FVZ	4FW0	4GQE
space group	$P2_12_12_1$	$P2_12_12_1$	$P2_12_12_1$	$P2_12_12_1$	$P2_12_12_1$	$P2_12_12_1$
cell dimensions						
a (Å)	52.1	52.0	51.9	51.9	52.1	52.0
b (Å)	111.0	111.3	110.9	110.8	111.3	111.1
c (Å)	165.3	165.1	164.5	164.5	164.1	164.3
resolution (Å)	1.80 (1.83−1.80)	2.00 (2.03−2.00)	1.70 (1.73−1.70)	2.00 (2.03−2.00)	1.95 (1.98−1.95)	1.78 (1.81−1.78)
R_{sym} or R_{merge}	0.077 (0.626)	0.071 (0.588)	0.055 (0.443)	0.075 (0.636)	0.064 (0.662)	0.057 (0.746)
$I/\sigma I$	29.9 (1.8)	19.7 (1.7)	31.8 (2.0)	23.3 (1.9)	24.3 (2.0)	31.6 (2.3)
no. of unique reflections	88431	65282	102661	65397	70555	88147
completeness (%)	99.6 (99.9)	99.6 (97.8)	97.5 (99.2)	99.4 (99.9)	99.6 (99.9)	99.4 (98.7)
redundancy	4.2 (3.6)	4.0 (3.6)	5.0 (4.6)	3.8 (3.8)	4.0 (4.0)	4.5 (3.8)
			Refinement			
resolution (Å)	1.81	2.00	1.70	2.00	1.95	1.80
no. of reflections used	83967	61988	97474	61954	66998	83676
R_{work}/R_{free} [b]	0.181/0.218	0.181/0.221	0.184/0.212	0.202/0.248	0.194/0.232	0.189/0.222
mean *B* value (Å^2)	48.03	47.98	36.52	52.98	43.26	46.80
no. of atoms						
protein	6687	6659	6679	6667	6655	6662
ligand/ion	171	165	157	160	167	153
water	374	388	419	262	322	380
root-mean-square deviation						
bond lengths (Å)	0.013	0.013	0.012	0.015	0.013	0.013
bond angles (deg)	2.019	1.424	1.303	1.522	1.352	2.051

[a]See Figure 1 for nomenclature and chemical formulas of NHA analogues. [b]R_{free} was calculated with the 5% of reflections set aside throughout the refinement. The set of reflections for the R_{free} calculation was kept the same for all data sets according to those used in the data of the starting model (PDB entry 1OM4).

Luna C18 column was used with water as solvent A and acetonitrile as solvent B. A gradient from 10 to 90% B was run over 30 min at a rate of 1.0 mL/min. DNPH derivatives were detected at 360 nm. Under these conditions, DNPH eluted at 12.2 min and DNPH−formaldehyde eluted at 13.3 min (DNPH−acetaldehyde, 14.2 min; DNPH−acetone, 14.9 min). A DNPH−formaldehyde standard curve (R^2 = 0.995) was linear from 100 μM to 1.5 mM.

HPLC MS Confirmation of NDA and DNPH Derivatives. The identities of all NDA- and DNPH-derivatized products of the [^{14}C]NMOA reactions were confirmed by liquid chromatography and mass spectrometry (LC−MS) using an Agilent 1200 series purification system equipped with a diode array detector (SL 1315C) set to 460 (or 360) and 254 nm and an Agilent 6130A Single Quad detector using atmospheric-pressure electrospray ionization (API-ES) in positive mode. A Phenomenex Gemini-NX C18 (4.6 mm × 50 mm, 5 μm, 100 Å) column was used with solvent A as LC−MS grade water with 0.1% formic acid and solvent B as LC−MS grade ACN with 0.1% formic acid. For NDA derivatizations, the following gradient was run at a flow rate of 1.5 mL/min: 5 to 50% B from 0 to 7 min and 100% B from 7 to 10 min. Derivatives had the following retention times: NDA−NHA, 4.2 min; NDA−citrulline, 6.2 min; NDA−NMOA, 4.4 min; NDA−NHMA, 4.4 min; NDA−NMMA, 4.6 min. For DNPH derivatizations, the following gradient was used: at a flow rate of 1.5 mL/min, from 0 to 10 min, 10 to 90% B. DNPH−formaldehyde eluted at 3.26 min under these conditions.

Determination of Crystal Structures. The heme domain of the rat nNOS protein sample and crystals were prepared according to the procedures reported previously.[36] Fresh crystals (1−2 days old) were first passed stepwise through cryoprotectant solutions[36] and then soaked with 10 mM NHA analogues for 4−6 h at 4 °C before being mounted on nylon loops and flash-cooled by being plunged into liquid nitrogen.

The cryogenic (100 K) X-ray diffraction data were collected remotely at various beamlines at the Stanford Synchrotron Radiation Lightsource or Advanced Light Source through the data collection control software and a crystal mounting robot. Raw data frames were indexed, integrated, and scaled using HKL2000.[37] The binding of NHA analogues was detected by the initial difference Fourier maps calculated with REFMAC.[38] The analogue molecules were then modeled in COOT[39] and refined using REFMAC. Water molecules were added in REFMAC and checked through COOT. The TLS protocol[37,40] was implemented in the later stage of refinements with each subunit as one TLS group. Finally, an additional round of TLS refinement was conducted with the coordinates of the substrate analogue and the water of interest removed from the input model. The map coefficients in the output were used to produce the omit $F_o - F_c$ electron density maps shown in Figure S11 of the Supporting Information. The refined structures were validated through the RCSB web server before being deposited in the Protein Data Bank (PDB). The crystallographic data collection and structure refinement

dx.doi.org/10.1021/bi301571v | Biochemistry 2013, 52, 3062−3073

statistics are summarized in Table 1 with PDB entry codes included.

MeOX and FDH Reactions. MeOX and FDH were obtained from Sigma-Aldrich (catalog nos. A2404 and F8649, respectively). Ten microliters of 80 units/mL MeOX in 100 mM HEPES (pH 7.5) was reacted with 100 μL of sample (methanol standards or iNOS–substrate reaction mixtures) for 1 h at room temperature. MeOX reactions with methanol standards followed by DNPH derivatization and HPLC separation produced a standard curve (R^2 = 0.89) with a detection limit of 100 μM. [^{14}C]NMOA–iNOS reaction mixtures incubated with MeOX were DNPH-derivatized (see Materials and Methods) and analyzed by HPLC and scintillation counted. Reactions longer than 1 h did not show stoichiometric turnover.

In a 20 mL glass scintillation vial, the following compounds were combined: 100 μL of [^{14}C]NMOA–iNOS reaction mixture, 10 μL of 80 units/mL MeOX, and 10 μL of 80 units/mL FDH. The vial was sealed with a septum containing a suspended 1 mL plastic well. The contents of the vial were reacted for 12 h at room temperature. Using a syringe, 200 μL of an 8% (v/v) aqueous solution of NaOH was carefully added to the plastic well and 200 μL of a 20% (v/v) aqueous solution of TCA was added to the multienzyme reaction mixture in the bottom of the vial. The vial was further incubated at 37 °C while being gently shaken for 2 h. The suspended reaction well was carefully separated from the vial, and each was scintillation counted. Figure S10 of the Supporting Information shows the chromatograms for those experiments.

RESULTS

Synthesis of the NHA Analogues. NMOA, NEOA, NHMA, and NMMA were synthesized through nucleophilic addition of appropriate amines to a protected ornithine thiourea (see Scheme S1 of the Supporting Information).[24,41] MHA was synthesized by the procedure of Clement and co-workers.[42] tBOA was synthesized as previously described and was purified by HPLC.[22]

Kinetic Evaluation of NHA Analogues. The production of NO from iNOS and nNOS was evaluated using the hemoglobin capture assay, which monitors the absorbance increase at 401 nm as the methemoglobin is produced.[31] Figure 2 shows Michaelis–Menten curves for NHA analogues that behave as substrates. Table 2 reports kinetic values for the compounds measured. Figure S1 of the Supporting Information provides the individual Michaelis–Menten curves used for the determination. The mechanism is thought to be highly conserved among NOS isoforms. In many cases, we examine both isoforms, while in other experiments (such as crystal structure determination), we use only nNOS. Subtle mechanistic differences between NOS isoforms are not taken into account. Of the five NHA analogues studied, only NMOA and NHMA were found to produce NO. Overall, the substrates have a slightly greater affinity for nNOS than iNOS. Alternative substrates, NMOA and NHMA, produce NO with K_m values similar to that for NHA, but with lower k_{cat} (turnover) values; the k_{cat} for NMOA is ~4 and ~7 times lower and that for NHMA ~18 and ~13 times lower with iNOS and nNOS, respectively, than with NHA. Kinetic trends are the same for both NOS isoforms; for nNOS and iNOS, NMOA has a weaker binding affinity for the active site (higher K_m), but a greater rate of turnover (higher k_{cat}) than NHMA. An enzyme would likely be evolutionarily optimized for its native substrate, so the lower

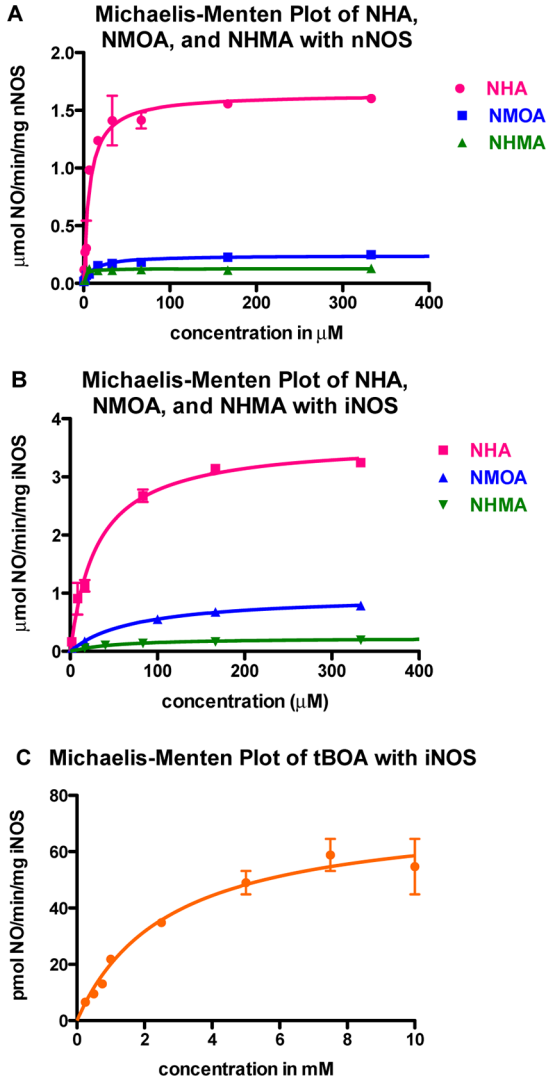

Figure 2. Michaelis–Menten curves of NHA, NMOA, and NHMA with (A) nNOS and (B) iNOS. (C) Michaelis–Menten curve of tBOA with iNOS. Note the different units along both axes. The corresponding Michaelis–Menten values are listed in Table 2.

enzyme efficiencies (k_{cat}/K_m) for these analogues are expected. The absence of NO production was confirmed for NEOA, NMMA, and MHA by longer incubations with iNOS (1, 2, 6, 12, and 24 h) using the Griess reagent.[31]

Spectral binding affinities (K_s) for iNOS were also determined (Table 2 and Figures S2–S8 of the Supporting Information) using the previously described spectral binding assay.[33] In this assay, imidazole, which coordinates directly to the heme iron causing a Soret shift, is first bound to NOS and then NHA analogues are titrated into the cuvette while the Soret shift are monitored as these compounds displace the imidazole (see Materials and Methods). Therefore, these values directly reflect the affinity the compound has for the active site. For the substrates, K_s values are similar to K_m values, as expected. For the compounds that are not substrates, the K_s values may rationalize why turnover cannot occur. MHA, for example, was found to have a very high K_s value, indicating its very poor binding affinity. This was confirmed upon analysis of the crystal structure (see below). NEOA and NMMA are not substrates but have good binding affinities, so other factors must be preventing these compounds from being substrates.

dx.doi.org/10.1021/bi301571v | Biochemistry 2013, 52, 3062–3073

Table 2. Kinetic Values Determined for NHA Analogues[a]

	NHA		NMOA		NHMA		NEOA	NMMA	MHA	tBOA[c]
	iNOS	nNOS	iNOS	nNOS	iNOS	nNOS	iNOS	iNOS	iNOS	iNOS
K_m (μM)	22 ± 5	5.7 ± 2.1	88 ± 8	11 ± 2	34 ± 6	2.0 ± 0.4	–	–	–	2.7 ± 0.8 mM
k_{cat} (min^{-1})	16 ± 2	13 ± 4	4.7 ± 1.3	1.8 ± 0.5	0.9 ± 0.5	1.0 ± 0.2	–	–	–	0.3 ± 0.1
k_{cat}/K_m ($\mu M\ min^{-1}$)	0.5	2.8	0.05	0.16	0.03	0.03	–	–	–	0.11
K_s (μM)	29 ± 4	–	122 ± 20	–	34 ± 4	–	120 ± 13	70 ± 5	>10 mM	–
K_i[b]	not available		not available		not available		26 ± 3 μM	28 ± 3 μM	>10 mM	7.4 ± 4.5 mM

[a]See the Supporting Information for Michaelis–Menten plots (Figure S1) and inhibition curves and difference spectra (Figures S2–S9). [b]All compounds were also evaluated as inactivators, but none was found to cause time-dependent inhibition (see Figure S9 of the Supporting Information). [c]The k_{cat} value differs from that previously reported;[22] the same enzyme concentration was used here for all of the compounds, which is lower than that used in the earlier publication for tBOA, so that all data in this table could be meaningfully compared.

Inhibition constants (K_i) with iNOS were determined for those compounds that were not substrates (Table 2 and Figure S9 of the Supporting Information). Slow substrates will also be competitive inhibitors, but measuring a K_i value is not meaningful because slower, alternate substrate turnover is also occurring. For the four compounds for which K_i values are meaningful (NEOA, NMMA, MHA, and tBOA), and therefore reported, these values agree with binding affinity (K_s) values. The K_i and the K_s for MHA are both very high (>10 mM), while the K_i values for NEOA and NMMA are midmicromolar. K_i values also indicate competition with arginine, thereby confirming that the analogues are inhibiting NOS at its active site.

We also re-evaluated tBOA, a previously reported weak NOS substrate. It has a poor binding affinity for iNOS, evidenced by its K_i value of 7.4 mM and its K_m value of 2.7 mM. tBOA has the slowest k_{cat}, approximately one-third the rate of NHMA, the slowest of our NHA analogues for iNOS.

The NHA analogues were also evaluated as time-dependent inactivators of iNOS. In all cases, NOS activity was fully restored by addition of L-arginine to preincubations of each compound with iNOS under turnover conditions, indicating that time-dependent inactivation was not occurring (Figure S9C of the Supporting Information).

Citrulline Production. For substrates NMOA and NHMA, the amino acid product was confirmed to be solely citrulline (chromatographs are shown in Figure S13 of the Supporting Information). This was done by naphthalene-2,3-dicarboxyaldehyde (NDA) derivatization of the products of NOS (both iNOS and nNOS were used and experiments performed in at least triplicate) reactions with subsequent HPLC separation and spectral detection at 460 nm (see Materials and Methods). An authentic standard of N^{ω}-cyanoornithine (CN-Orn) was prepared to confirm its absence from all of the analogue–NOS reactions.

NADPH Consumption and NO Production. The rates of production of NO and consumption of NADPH were compared for all substrates (Table 3) with iNOS. NO production was measured using the hemoglobin capture assay, monitoring methemoglobin formation at 401 nm, while simultaneously measuring the conversion of NADPH to $NADP^+$ at 340 nm. Table 3 shows that arginine and NHA consume approximately 1.5 and 0.5 equiv, respectively, of NADPH for each NO molecule released. NMOA and NHMA, however, consume many more equivalents of NADPH (8 and 15, respectively) than the number of equivalents of NO produced. This result is consistent with the slower k_{cat} values (Table 2) for these two analogues when compared to that of NHA; NMOA and NHMA are not efficient substrates for NOS.

Table 3. Uncoupling of NO Production from NADPH Consumption

substrate	arginine	NHA	NMOA	NHMA
NADPH:NO ratio[a]	1.7 ± 0.2	0.7 ± 0.3	8.0 ± 1.5	15.0 ± 2.7

[a]Ratios are expressed as moles of NADPH consumed per mole of NO formed with iNOS, averaged over five or more experiments.

Identification of the One-Carbon Metabolite of NMOA. NOS turnover of NMOA produces citrulline and NO, leaving the methyl of the N^{ω}-methoxyl group unaccounted for. To address this issue, N^{ω}-[^{14}C]methoxy-L-arginine ([^{14}C]NMOA) was synthesized using the chemistry shown in Scheme S1 of the Supporting Information,[24,41] with the exception that [^{14}C]methoxylamine (34 mCi/mmol) was used as the amine added to the activated thiourea [**2** (Scheme S1 of the Supporting Information)].

Reactions of iNOS with [^{14}C]NMOA, NMOA, or NHA or without a substrate were (1) analyzed by NDA derivatization and HPLC separation to quantify amino acids, (2) analyzed by 2,4-dinitrophenyl hydrazine (DNPH) derivatization and HPLC separation to identify aldehydes and ketones, and (3) allowed to proceed with methanol oxidase and formate dehydrogenase to convert methanol into formaldehyde and formate and to convert formate into bicarbonate, respectively (Scheme 3). Before HPLC analysis, reaction mixtures were filtered through a 10000 MWC filter. Filters were found to contain no ^{14}C, indicating that covalent modification of the enzyme is not occurring.

NDA derivatization of the [^{14}C]NMOA–iNOS reaction mixture was conducted by HPLC and scintillation counted (see Figure S10 of the Supporting Information). These spectra show that the only ^{14}C species to elute, in addition to [^{14}C]NMOA, is located in the early fractions (2–4 min), suggesting that this metabolite is highly polar. We hypothesize that this is a one-carbon metabolite from the [^{14}C]NMOA–iNOS reaction. DNPH was next used to detect aldehydes and ketones from the iNOS reactions in search of formaldehyde as a potential one-carbon byproduct of [^{14}C]NMOA–NOS metabolism. With an excess of DNPH, no significant amount of ^{14}C eluted with DNPH–formaldehyde standards, indicating that the one-carbon metabolite from these reactions is not formaldehyde.

Numerous attempts to detect methanol directly by chromatography or mass spectrometry were unsuccessful, which excluded experiments conducted in isotopic water or oxygen. Consequently, enzymatic conversion was employed to convert any methanol produced to formaldehyde, then to

dx.doi.org/10.1021/bi301571v | Biochemistry 2013, 52, 3062–3073

Scheme 3. Flowchart of Enzyme Reactions and Detection Methods Used in the Determination of the One-Carbon Metabolite of NMOA

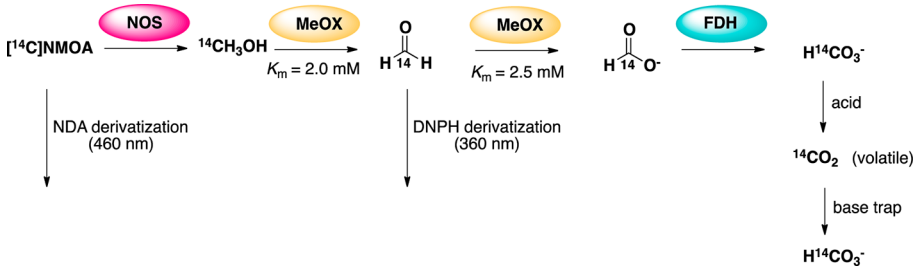

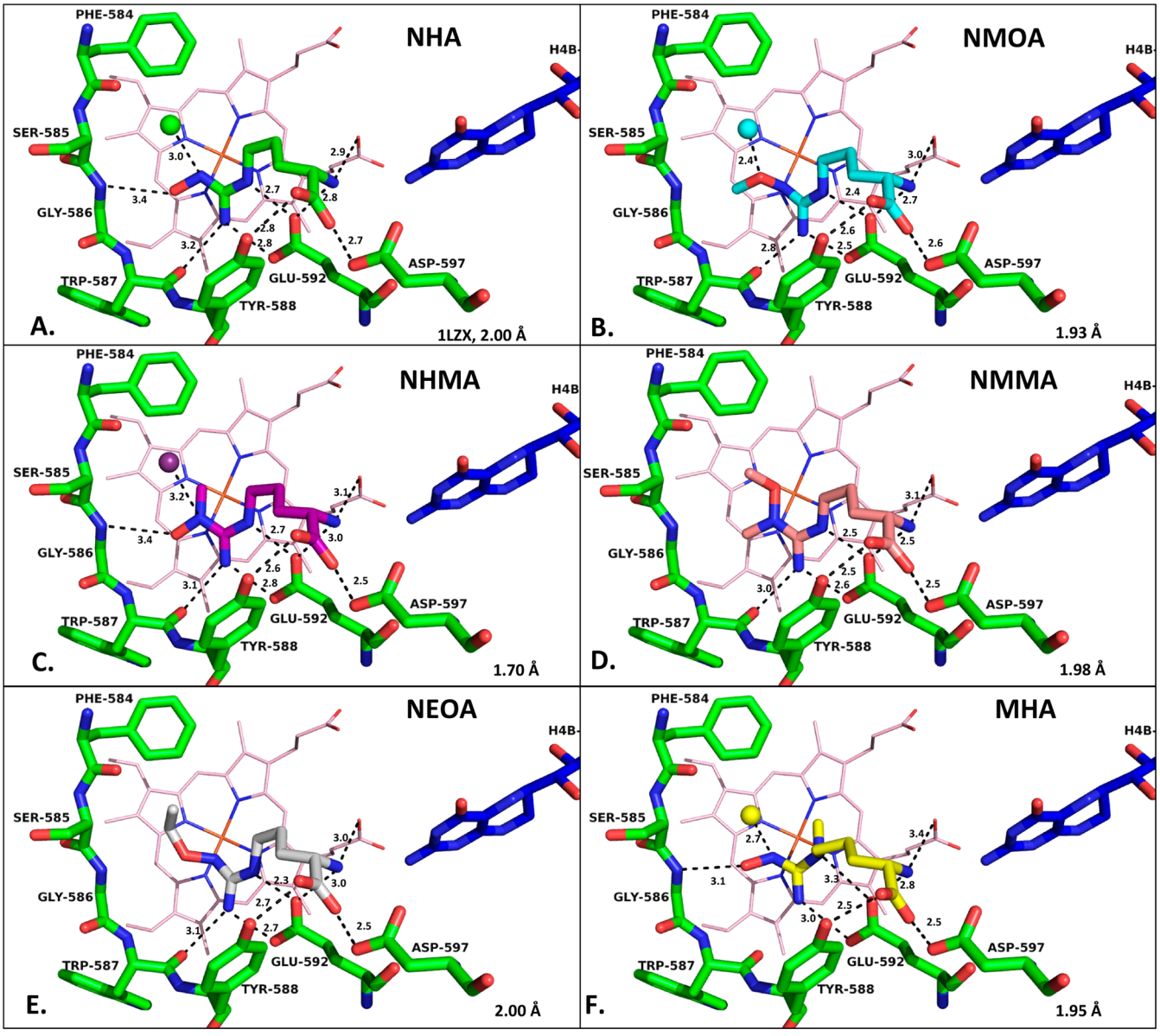

Figure 3. Crystal structures of analogues in complexes with nNOS. Heme is colored light pink and H_4B dark blue. nNOS active site residues are colored green. The active site water is shown as a sphere: (A) NHA (green, PDB entry 1LZX), (B) NMOA (cyan), which was modeled with the methyl group in two alternate positions but with only major one shown, (C) NHMA (magenta), (D) NMMA (peach), (E) NEOA (gray), and (F) MHA (yellow), which showed poorer density quality indicating partial disordering. Hydrogen bonding interactions are depicted as black dashed lines; distances are reported in angstroms. See Figure S12 of the Supporting Information for the crystal structure of tBOA.

formic acid, and then to carbon dioxide, as depicted in Scheme 3. Methanol oxidase (MeOX) converts methanol to formaldehyde and H_2O_2 with a K_m of approximately 2 mM (depending on the O_2 concentration) but also catalyzes the conversion of formaldehyde to formate with a K_m of 2.5 mM.[43] Following reaction with MeOX, [^{14}C]NMOA−iNOS reactions

dx.doi.org/10.1021/bi301571v | *Biochemistry* 2013, 52, 3062−3073

produced small amounts of [^{14}C]DNPH−formaldehyde, but amounts that were stoichiometrically smaller than the amount of citrulline produced by the same reactions in the absence of MeOX, because of the conversion of some of the produced formaldehyde to formate by MeOX. To better quantify methanol formation in the iNOS-catalyzed reaction, [^{14}C]NMOA was incubated with a mixture of iNOS, MeOX, and formate dehydrogenase (FDH); FDH converts the formate produced in the MeOX reaction to bicarbonate, which, after acidification, produces carbon dioxide, which can be trapped in a base, allowing for quantitative detection of all of the ^{14}C metabolites as DNPH−formaldehyde and CO_2. Experiments repeated with MeOX but without FDH did not produce [^{14}C]CO_2, confirming the identity of the one-carbon metabolite of the [^{14}C]NMOA−iNOS reaction as [^{14}C]methanol exclusively.

Crystal Structures of the Substrate Analogues. Crystal structures of substrate analogues bound to the rat nNOS oxygenase domain were obtained (Figure 3 and omit electron densities in Figure S11 of the Supporting Information). Similar to NHA and arginine, all analogues retain the four hydrogen bonds conserved for an L-amino acid moiety: amino acid COO^- to Tyr588 OH, amino acid COO^- to Asp597 COO^-, amino acid NH_3^+ to Glu592 COO^-, and amino acid NH_3^+ to heme propionate A. The planarity of the guanidino group is, more or less, maintained for all compounds but MHA. This planarity allows the two guanidino nitrogens, N^{δ} and $N^{\omega\prime}$, to hydrogen bond to Glu592. These key interactions place the guanidino head over the heme for potential catalysis. However, with MHA, the presence of an N^{δ}-methyl destroys the planarity of guanidine, resulting in only one hydrogen bond from $N^{\omega\prime}$ to Glu592. The short distance (~3.9 Å) from the extra N^{δ}-methyl to heme could be sterically preventing O_2 from binding to the heme iron, thus preventing turnover. Steric blockage of productive oxygen binding was hypothesized to be the reason that arginine and NHA analogues bearing a C5 methyl substitution at the *pro-R* position are not substrates.[19] The electron density for MHA is the poorest of those five analogue structures, which reflects unfavorable interactions between the distorted guanidino group of MHA and the NOS active site and is consistent with the poor binding affinity determined for this compound (see Table 2).

Similar to NHA, the N^{ω}-OH group of NHMA and MHA forms a weak hydrogen bond to the backbone nitrogen of Gly586 (Figure 3). Any substituent on this hydroxyl group would eliminate this hydrogen bond by either dragging the oxygen atom away from Gly586 as in NEOA, totally swinging away as in NMMA, or being blocked by a methyl group as in NMOA (Figure 3). The orientation and bulkiness of this substituted hydroxyl will, in turn, influence whether an active site water molecule can bind next to the analogue. The active site water usually hydrogen bonds to the substrate N^{ω} atom. This hydrogen bonding interaction is maintained in NHMA and is at least partially retained in MHA and NMOA via the oxygen atom from the analogue. In MHA, the water molecule is not fully occupied because of the closeness of the hydroxyl group, while in NMOA, the methyl of the methoxyl moiety adopts two conformations, where the predominant conformation, shown in Figure 3B, allows for a partially occupied water molecule that shares the same space with the methyl group in its minor conformation (Figure S11A of the Supporting Information). However, in NEOA or NMMA, either an ethyl or a methyl group, respectively, occupies the space of the active site water. In the nitric oxide ferrous complex of nNOS, this same water molecule is within hydrogen bonding distance of the O atom of NO and thus is in an ideal position to serve as a proton donor.[20]

We also have obtained a crystal structure of tBOA in the active site of nNOS (see Figure S12 of the Supporting Information). There is no water molecule present in the active site in this cocrystal structure. The *tert*-butyl group is apparently too bulky to fit in the site and is, therefore, disordered; the three *tert*-butyl methyl groups exchange their positions but are populated more in the space that a water molecule normally occupies. Therefore, there is no active site water molecule present even though this compound is a weak substrate.

DISCUSSION

The products of NOS turnover with the various NHA analogues were investigated. Citrulline is the only amino acid product formed from NMOA and NHMA. In addition to citrulline, NOS produces CN-Orn when NHA is the substrate and when H_2O_2 is used in place of NADPH.[44] It is thought that citrulline is the product of native NOS−NHA chemistry (through the ferric peroxo intermediate), while CN-Orn is the product of non-native NOS−NHA chemistry, when NOS is forced to go through CpdI.[10] Because citrulline is the only amino acid product of NMOA and NHMA, this suggests NOS is performing native chemistry through $Fe^{III}OO^-$/$Fe^{III}OOH$, not through CpdI, on these substrates.

There is significantly more consumption of NADPH per NO released for substrates NMOA and NHMA (8 and 15 equiv, respectively) than for L-arginine and NHA (1.5 and 0.5 equiv, respectively). These ratios were measured at substrate concentrations approximately equal to their K_m values. Uncoupling of substrate turnover from electron consumption happens when superoxide ($O_2^{\bullet-}$) is released from the ferric superoxide complex [$Fe^{III}OO\bullet$ (see Scheme 2)] before substrate modification. This unproductive consumption of electrons by NOS occurs at subsaturating concentrations of L-arginine or H_4B.[6,35] Uncoupling also occurs in the presence of alternate substrates such as homoarginine[45] or inactivators such as N^5-(1-iminoethyl)-L-ornithine,[46] suggesting substrate identity affects the feasibility of oxidation. *Bacillus subtilis* NOS Trp66 (the Trp residue that hydrogen bonds to H_4B) mutants also show uncoupling.[47] This demonstrates the importance of the entire NOS enzyme structure in implementing efficiently coupled substrate turnover and that even seemingly small, single-residue changes can largely affect enzymatic outcomes. Both substrates, NMOA and NHMA, show some uncoupling during turnover, which means NADPH reducing equivalents may be used for the production of other products, such as superoxide, rather than NO (Table 3). A highly coupled system requires precise proton transfer steps, and therefore, those substrates that are uncoupled, very likely, perturb the local proton transfer mechanism. It should be noted that substrate oxidation is a multistep process and that alternative substrates may potentially affect other steps, for example, the transfer of an electron from the reductase. Furthermore, the consistency between low k_{cat} values (Table 2) and higher uncoupling for NMOA and NHMA suggests that oxidation of these alternative substrates represents only 5−10% of iNOS catalysis. The decrease in k_{cat} (approximately 5 and 10% of the k_{cat} of NHA) could be the result of this dramatic degree of uncoupling.

The one-carbon metabolite of [^{14}C]NMOA was found to be methanol. This differs from the one-carbon metabolite

determined to be present in NOS−NHMA reactions; Olken and Marletta found that NHMA produces formaldehyde, first going through NHA as an intermediate.[26] The stronger uncoupling (Table 3) of NHMA compared to that of NMOA is consistent with the fact that NHMA processing requires an additional oxidation step to yield the observed formaldehyde. This suggests that different substrates are metabolized by NOS through different mechanisms.

We have previously reported[22] that both N^{ω}-*tert*-butyloxy-L-arginine and N^{ω}-(3-methyl-2-butenyl)oxy-L-arginine are NOS substrates; therefore, a direct abstraction of a hydrogen atom from the N^{ω} hydroxyl does not appear to be required in the second step of the NOS reaction for these two alternative substrates. It, therefore, may seem surprising that NHMA is a NOS substrate because NHMA lacks the N^{ω} proton. In light of this, we propose that at least one of the two protons, either N^{ω}-H or N^{ω}O-H, is necessary for turnover. The positions of these protons are seemingly interchangeable because of the conformational isomers that exist, and either may be functioning as a proton source during oxygen activation (see Figure 4A). Density functional theory calculations suggest that

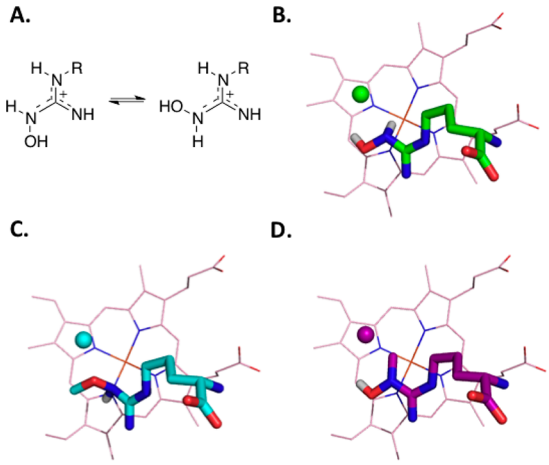

Figure 4. (A) Conformational isomers of NHA analogues. (B) Crystal structure of NHA (green) with N^{ω}-H and N^{ω}-OH (white) rendered. (C) Crystal structure of NMOA (cyan) with N^{ω}-H (white) rendered. The methyl of the methoxyl group occupies two alternate positions, but only one is shown here. (D) Crystal structure of NHMA (magenta) with N^{ω}-OH (white) rendered. In all panels, heme (light pink) is shown as lines; NHA and analogues are shown as sticks and active site water molecules as spheres. Rendered protons are colored white, nitrogens blue, and oxygens red. The colors of carbon atoms are specified for each substrate.

both are comparable in energy for hydrogen atom donation.[21] Crystal structures typically reflect the most stable binding conformation but do not reveal other possible conformations that may exist under the dynamic conditions of an enzyme active site. By comparison of the crystal structures for the three substrates, along with their turnover rates, we hypothesize that deprotonation at N^{ω}-H is favored on the basis of its physical proximity to the heme iron and the slower k_{cat} for NHMA versus that for NMOA (Table 2). While even the native substrate (NHA) may go through many pathways, this suggests that N^{ω}-H, positioned down toward the heme iron (Figure 4B,C), is more easily removed, but that N^{ω}O-H, positioned farther from the heme iron (Figure 4B,D), can also serve as a viable proton source, but less efficiently. The substrate might rotate around the C−N bond for N^{ω}O-H to be aligned for deprotonation, but because this is not the conformation depicted in the crystal structure, it is likely not the most energetically favorable conformation. The fact that NMMA, a compound in which both N^{ω}-H and N^{ω}O-H are replaced with methyl groups, has good binding affinity for the NOS active sites but is not a NOS substrate is consistent with our hypothesis that the presence of at least one N^{ω} proton is essential for turnover.

Previous ENDOR and X-ray experiments, as well as DFT calculations, show that NHA is most likely protonated in the active site.[21] The existence of a water molecule next to the guanidino group of the substrate could play a role in maintaining its protonated state, thus affecting the rate of catalysis. On the basis of the substrate activities of NMOA and NHMA, and the lack of activity with NMMA, we propose a possible mechanism for the reaction of NOS with NHA and NMOA (Scheme 4). The turnover and one-carbon metabolite of NHMA have been previously examined in detail.[26] As shown in Scheme 4, the ferric superoxide heme species is activated upon receiving an electron from H_4B. The resulting ferric peroxide species is then protonated by the substrate to form the reactive ferric hydroperoxide species. On the basis of experimental evidence supporting $Fe^{III}OOH$ as the active species,[15] and our results suggesting the necessity of the active site proton, we hypothesize that $Fe^{III}OOH$ needs to be formed to create the proper "push−pull" dynamics and electronics for the reaction to occur. The ferric hydroperoxide then undergoes an attack on the electrophilic guanidinium carbon. Driven by the formation of citrulline, this tetrahedral intermediate collapses, producing a protonated or methylated nitric oxide species, which is subsequently processed, aided via appropriate proton transfers by the active site water molecule. A heme−NO complex forms, which donates an electron back to the radical cation of H_4B to produce H_4B, NO, and ferric heme. This proposed mechanism invokes the active site water in the processing of the released NO-containing product; however, additional roles, such as other proton transfers, structural stability, or pK_a maintenance, are also possible.

Because both NMOA and NHMA are NOS substrates, but NMMA is not, it is reasonable to conclude that NOS can process a singly methylated NO species, but not a doubly methylated species. However, although the proton is necessary, it is not sufficient, as NEOA has N^{ω}-H available but is not a substrate. We can account for this by considering two mechanistic pathways. (1) In a nucleophilic pathway, as shown in Scheme 4, an N^{ω}O-ethyl species may be too sterically hindered to undergo reaction, while methyl-N^{ω}O and N^{ω}O-methyl species are more reactive and can be processed by NOS. (2) In an electrophilic cleavage of the N^{ω}O−R bond, it would be expected that none of the small alkyl-substituted analogues would be likely to be cleaved because of the high energy of the resulting cation. N^{ω}-*tert*-Butyloxy-L-arginine and N^{ω}-(3-methyl-2-butenyl)oxy-L-arginine,[22] however, are substrates, which argues in favor of the second mechanism and against the first. According to the second mechanism, the stability of the resulting cations (*tert*-butyl and dimethylallyl, respectively) might suggest that these compounds should be excellent substrates, but they are only weak substrates.[22] The crystal structures of NEOA (Figure 3E) and tBOA (Figure S12 of the Supporting Information) show that there is no active site water molecule bound; the bulky hydrophobic substituents apparently displace it. However, whereas NEOA is not a substrate,

dx.doi.org/10.1021/bi301571v | *Biochemistry* 2013, 52, 3062−3073

Scheme 4. NOS Turnover of NHA and NMOA

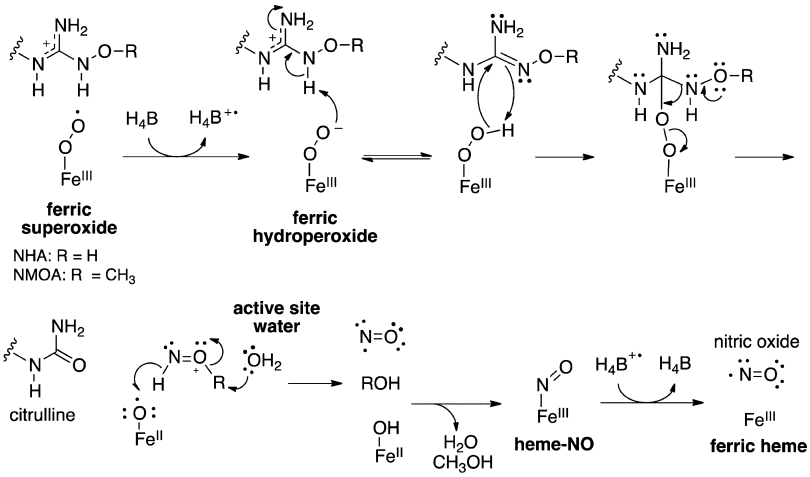

Scheme 5. Pathway by Which tBOA Could Be Acting as a Substrate despite the Lack of an Active Site Water Molecule

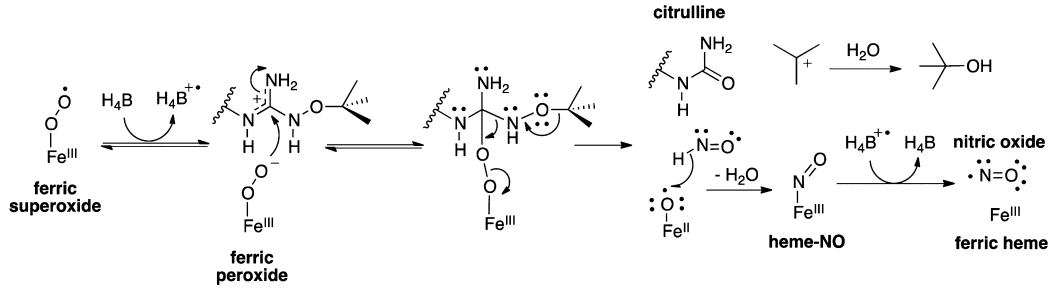

tBOA is a substrate, suggesting that the water molecule may not be essential for activity and, perhaps more importantly, that there is likely more than one mechanism by which substrates can be turned over. Perhaps, substrates with larger substituents that displace the water molecule but can form stabilized carbocations are metabolized through a mechanism that does not require a water molecule, a mechanism in which the transfer of an electron from the H_4B to ferric superoxide occurs initially followed by the attack of ferric peroxide on the substrate (Scheme 5). Because of the stability of the resulting carbocation, spontaneous breakdown of the tetrahedral intermediate gives citrulline, HNO, and ferrous oxo radical. Abstraction of a hydrogen atom from HNO by $Fe^{II}O$ with loss of water produces the heme−NO complex. As shown in Scheme 4, the radical cation of H_4B accepts an electron to give NO and ferric heme. In the case of NEOA, the water molecule is displaced, but because an ethyl cation is not sufficiently stable, breakdown of the second intermediate does not occur and the equilbrium favors substrate.

In the unique case of MHA bound to nNOS, an active site water, at least partially, exists and both N^{ω} protons are present, but this compound is not a substrate. In the crystal structure (Figure 3F), the N^{δ}-methyl distorts the planarity of the guanidino group, thereby weakening its crucial interactions with Glu592, which contributes to its poor binding affinity. The close positioning of this N^{δ}-methyl to the heme iron (~3.9 Å) could prevent productive binding of molecular oxygen.

The role of the active site water in the second step of NOS catalysis is still quite controversial. Marletta and co-workers cleverly examined C5-methylated arginine and NHA analogues, finding that N^{ω}-hydroxy-(5*S*)-methyl-L-arginine is a NOS substrate while (5*S*)-methyl-L-arginine is not.[19] They speculated that both analogues bearing a (5*S*)-methyl substituent displace the active site water molecule. On the basis of their modeling results, they suggested that the active site water is required for the first step of NOS catalysis but is not required for the second step. The NHA analogue crystal structures presented here (Figure 2) show that, when present, the active site water molecule does not bind near C5 but interacts with N^{ω} near Ser585, and MHA, which has an N^{δ}-methyl substituent, still binds with an active site water molecule (Figure 3F). On the basis of our crystal structures, it is possible that (5*S*)-methyl compounds also would allow active site water binding; further structural data are needed to confirm this hypothesis. However, as supported by the example of tBOA, this water molecule cannot be deemed essential for catalysis with all NHA analogues; our results suggest it does play a role in the turnover of NHA, NMOA, and NHMA.

Our findings suggest that substrate identity, especially its steric bulkiness, dictates the ability of a water molecule to bind in the active site; if the water is involved in the predominant turnover pathway, its binding could determine the ability of NOS to catalyze a reaction on a substrate and determine the rate of catalysis. A caveat to this hypothesis arises because our crystal structures do not contain a heme oxo species; substrates would be repositioned when O_2 binds, and/or the O_2 ligand must bend in a different direction than we have observed in the NO complexes of nNOS and eNOS. When NO coordinates to the heme iron in nNOS, the substrate, L-arginine, must move ~0.7 Å.[20] The substrates under investigation in this study are larger, causing greater steric restriction for O_2 binding, and hence must move to allow O_2 to bind. Even so, there still should be sufficient room for the "catalytic" water to remain in

dx.doi.org/10.1021/bi301571v | *Biochemistry* 2013, 52, 3062−3073

place and provide a potential proton source for catalysis in the cases of NMOA and NHMA.

Compared to their substrate-promiscuous cytochrome P450 relatives, NOSs are very specific enzymes because of their more rigid, highly conserved active sites. An intricate set of hydrogen bond interactions holds substrates in the active site. The research described here demonstrates that NOS can metabolize several different substrates and may proceed through different mechanisms during metabolism of these various substrates.

In summary, we demonstrate that NOS can metabolize NHA analogues having a methyl substituted for either N^{ω}-H (NHMA) or N^{ω}-OH (NMOA), but not both (NMMA), and this is consistent with the importance of either N^{ω}-H or N^{ω}-OH in catalysis. Crystal structures reveal the presence of an active site water molecule that could also serve as a proton donor during substrate turnover, but *tert*-butoxy-L-arginine acts as a substrate, even though the *tert*-butyl group displaces the active site water, as shown in the crystal structure. We propose potential, alternative pathways (Schemes 4 and 5) consistent with our findings for these analogues as NOS substrates. Our crystal structures demonstrate that substrate identity dictates the presence or absence of the active site water molecule, but this does not always dictate substrate turnover. As a unique and complex enzyme, NOS not only is able to achieve two different oxygenation chemistries (step 1 and step 2) within its active site but also is flexible enough to oxidize various substituted NHA analogues, possibly by more than one mechanism.

■ ASSOCIATED CONTENT

Supporting Information

Synthetic methods, substrate and inhibitor plots, ^{14}C labeling methods, crystal structure information, MeOX and FDH reactions, HPLC−MS confirmation of NDA and DNPH derivatives, and NMR spectra of final products. This material is available free of charge via the Internet at http://pubs.acs.org.

Accession Codes

†Coordinates have been deposited with the Protein Data Bank (entries 4FVW for nNOS−NMOA, 4FVX for nNOS−NEOA, 4FVY for nNOS−NHMA, 4FVZ for nNOS−NMMA, 4FW0 for nNOS−MHA, and 4GQE for nNOS−tBOA).

■ AUTHOR INFORMATION

Corresponding Author

*R.B.S.: e-mail, Agman@chem.northwestern.edu; phone, (847) 491-5653. T.L.P.: e-mail, poulos@uci.edu; phone, (949) 824-7020.

Funding

This work was funded by National Institutes of Health (NIH) Grants GM049725 to R.B.S. and GM057353 to T.L.P. We thank Dr. Bettie Sue Siler Masters (NIH Grant GM52419, with whose laboratory P.M. and L.J.R. are affiliated). Dr. Bettie Sue Siler Masters also acknowledges the Welch Foundation for a Robert A. Welch Distinguished Professorship in Chemistry (AQ0012). P.M. is supported by Grant 0021620849 from MSMT of the Czech Republic. Support for K.J.L. was provided by Reach for the Stars, a GK-12 program supported by the National Science Foundation via Grant DGE-0948017.

Notes

The authors declare no competing financial interest.

■ ACKNOWLEDGMENTS

We thank the SSRL and ALS beamline staff for their support during remote X-ray diffraction data collection. We thank Dr. Jinwen Huang for synthesizing the NEOA.

■ ABBREVIATIONS

NOS, nitric oxide synthase; NO, nitric oxide; NHA, N^{ω}-hydroxy-L-arginine; nNOS, neuronal nitric oxide synthase; eNOS, endothelial nitric oxide synthase; iNOS, inducible nitric oxide synthase; H_4B, (6*R*)-5,6,7,8-tetrahydrobiopterin; CYP450, cytochrome P450; CpdI, compound I; tBOA, N^{ω}-*tert*-butyloxy-L-arginine; NMOA, N^{ω}-methoxy-L-arginine; NEOA, N^{ω}-ethoxy-L-arginine; NHMA, N^{ω}-hydroxy-N^{ω}-methyl-L-arginine; MHA, N^{δ}-methyl-N^{ω}-hydroxy-L-arginine; NMMA, N^{ω}-methoxy-N^{ω}-methyl-L-arginine; δMA, N^{δ}-methyl-L-arginine; [^{14}C]NMOA, N^{ω}-[^{14}C]methoxy-L-arginine; CN-Orn, N^{δ}-cyanoornithine; NDA, naphthalene-2,3-dicarboxyaldehyde; DNPH, 2,4-dinitrophenylhydrazine; MeOX, methanol oxidase; FDH, formate dehydrogenase.

■ REFERENCES

(1) Griffith, O. W., and Stuehr, D. J. (1995) Nitric oxide synthases: Properties and catalytic mechanism. *Annu. Rev. Physiol. 57*, 707−736.

(2) Calabrese, V., Mancuso, C., Calvani, M., Rizzarelli, E., Butterfield, D. A., and Stella, A. M. G. (2007) Nitric oxide in the central nervous system: Neuroprotection versus neurotoxicity. *Nat. Rev. Neurosci. 8*, 766−775.

(3) Alderton, W. K., Cooper, C. E., and Knowles, R. G. (2001) Nitric oxide synthases: Structure, function and inhibition. *Biochem. J. 357*, 593−615.

(4) Zhou, L., and Zhu, D.-Y. (2009) Neuronal nitric oxide synthase: Structure, subcellular localization, regulation, and clinical implications. *Nitric Oxide 20*, 223−230.

(5) Förstermann, U., Pollock, J. S., Schmidt, H. H., Heller, M., and Murad, F. (1991) Calmodulin-dependent endothelium-derived relaxing factor/nitric oxide synthase activity is present in the particulate and cytosolic fractions of bovine aortic endothelial cells. *Proc. Natl. Acad. Sci. U.S.A. 88*, 1788−1792.

(6) Gorren, A. C. F., and Mayer, B. (2007) Nitric-oxide synthase: A cytochrome P450 family foster child. *Biochim. Biophys. Acta 1770*, 432−445.

(7) Stuehr, D. J., Wei, C.-C., Wang, Z., and Hille, R. (2005) Exploring the redox reactions between heme and tetrahydrobiopterin in the nitric oxide synthases. *Dalton Trans.*, 3427−3435.

(8) Stoll, S., NejatyJahromy, Y., Woodward, J. J., Ozarowski, A., Marletta, M. A., and Britt, R. D. (2010) Nitric oxide synthase stabilizes the tetrahydrobiopterin cofactor radical by controlling its protonation state. *J. Am. Chem. Soc. 132*, 11812−11823.

(9) Hurshman, A. R., and Marletta, M. A. (2002) Reactions catalyzed by the heme domain of inducible nitric oxide synthase: Evidence for the involvement of tetrahydrobiopterin in electron transfer. *Biochemistry 41*, 3439−3456.

(10) Woodward, J. J., Chang, M. M., Martin, N. I., and Marletta, M. A. (2009) The second step of the nitric oxide synthase reaction: Evidence for ferric-peroxo as the active oxidant. *J. Am. Chem. Soc. 131*, 297−305.

(11) Feldman, P. L., Griffith, O. W., and Stuehr, D. J. (1993) The surprising life of nitric-oxide. *Chem. Eng. News 71*, 26−38.

(12) Korth, H. G., Sustmann, R., Thater, C., Butler, A. R., and Ingold, K. U. (1994) On the mechanism of the nitric oxide synthase-catalyzed conversion of N^{ω}-hydroxyl-L-arginine to citrulline and nitric oxide. *J. Biol. Chem. 269*, 17776−17779.

(13) Pant, K., and Crane, B. R. (2006) Nitrosyl-heme structures of *Bacillus subtilis* nitric oxide synthase have implications for understanding substrate oxidation. *Biochemistry 45*, 2537−2544.

(14) Crane, B. R., Sudhamsu, J., and Patel, B. A. (2010) Bacterial nitric oxide synthases. *Annu. Rev. Biochem. 79*, 445−470.
(15) Davydov, R., Sudhamsu, J., Lees, N. S., Crane, B. R., and Hoffman, B. M. (2009) EPR and ENDOR characterization of the reactive intermediates in the generation of NO by cryoreduced oxy-nitric oxide synthase from *Geobacillus stearothermophilus*. *J. Am. Chem. Soc. 131*, 14493−14507.
(16) Giroud, C., Moreau, M. M., Mattioli, T. A., Balland, V., Boucher, J.-L., Xu-Li, Y., Stuehr, D. J., and Santolini, J. (2010) Role of arginine guanidinium moiety in nitric-oxide synthase mechanism of oxygen activation. *J. Biol. Chem. 285*, 7233−7245.
(17) Santolini, J. (2011) The molecular mechanism of mammalian NO-synthases: A story of electrons and protons. *J. Inorg. Biochem. 105*, 127−141.
(18) Daff, S. (2010) NO synthase: Structures and mechanisms. *Nitric Oxide 23*, 1−11.
(19) Martin, N. I., Woodward, J. J., Winter, M. B., Beeson, W. T., and Marletta, M. A. (2007) Design and synthesis of C5 methylated L-arginine analogues as active site probes for nitric oxide synthase. *J. Am. Chem. Soc. 129*, 12563−12570.
(20) Li, H., Igarashi, J., Jamal, J., Yang, W., and Poulos, T. L. (2006) Structural studies of constitutive nitric oxide synthases with diatomic ligands bound. *J. Biol. Inorg. Chem. 11*, 753−768.
(21) Tantillo, D. J., Fukuto, J. M., Hoffman, B. M., Silverman, R. B., and Houk, K. N. (2000) Theoretical studies on N^G-hydroxy-L-arginine and derived radicals: Implications for the mechanism of nitric oxide synthase. *J. Am. Chem. Soc. 122*, 536−537.
(22) Huang, H., Hah, J.-M., and Silverman, R. B. (2001) Mechanism of nitric oxide synthase. Evidence that direct hydrogen atom abstraction from the OH bond of N^G-hydroxyarginine is not relevant to the mechanism. *J. Am. Chem. Soc. 123*, 2674−2676.
(23) Komori, Y., Wallace, G. C., and Fukuto, J. M. (1994) Inhibition of purified nitric oxide synthase from rat cerebellum and macrophage by L-arginine analogs. *Arch. Biochem. Biophys. 315*, 213−218.
(24) Schade, D., Kotthaus, J., and Clement, B. (2008) Efficient synthesis of optically pure N^{ω}-alkylated L-arginines. *Synthesis 2008*, 2391−2397.
(25) Schade, D., Kotthaus, J., Klein, N., Kotthaus, J., and Clement, B. (2011) Prodrug design for the potent cardiovascular agent Nω-hydroxy-L-arginine (NOHA): Synthetic approaches and physicochemical characterization. *Org. Biomol. Chem. 9*, 5249−5259.
(26) Olken, N. M., and Marletta, M. A. (1993) N^G-Methyl-L-arginine functions as an alternate substrate and mechanism-based inhibitor of nitric oxide synthase. *Biochemistry 32*, 9677−9685.
(27) Luzzi, S. D., and Marletta, M. A. (2005) L-Arginine analogs as alternate substrates for nitric oxide synthase. *Bioorg. Med. Chem. Lett. 15*, 3934−3941.
(28) Kotthaus, J., Schade, D., Töpker-Lehmann, K., Beitz, E., and Clement, B. (2008) N^{δ}-Methylated L-arginine derivatives and their effects on the nitric oxide generating system. *Bioorg. Med. Chem. 16*, 2305−2312.
(29) Hevel, J. M., White, K. A., and Marletta, M. A. (1991) Purification of the inducible murine macrophage nitric oxide syntase: Identification as a falvoprotein. *J. Biol. Chem. 266*, 22789−22791.
(30) Roman, L. J., Sheta, E. A., Martásek, P., Gross, S. S., Liu, Q., and Masters, B. S. S. (1995) High-level expression of functional rat neuronal nitric oxide synthase in *Escherichia coli*. *Proc. Natl. Acad. Sci. U.S.A. 92*, 8428−8432.
(31) Hevel, J. M., and Marletta, M. A. (1994) Nitric-oxide synthase assays. *Methods Enzymol. 233*, 250−258.
(32) Cheng, Y.-C., and Prusoff, W. H. (1973) Relationship between the inhibition constant (K_i) and the concentration of inhibitor which causes 50% inhibition (I_{50}) of an enzymatic reactio. *Biochem. Pharmacol. 22*, 3099−3108.
(33) Martell, J. D., Li, H., Doukov, T., Martásek, P., Roman, L. J., Soltis, M., Poulos, T. L., and Silverman, R. B. (2010) Heme-coordinating inhibitors of neuronal nitric oxide synthase. Iron−thioether coordination is stabilized by hydrophobic contacts without increased inhibitor potency. *J. Am. Chem. Soc. 132*, 798−806.
(34) Silverman, R. B. (2002) *The Organic Chemistry of Enzyme-Catalyzed Reactions*, 2nd ed., pp 563−596, Academic Press, San Diego.
(35) Adak, S., Wang, Q., and Stuehr, D. J. (2000) Arginine conversion to nitroxide by tetrahydrobiopterin-free neuronal nitric-oxide synthase. Implications for mechanism. *J. Biol. Chem. 275*, 33554−33561.
(36) Li, H., Shimizu, H., Flinspach, M. L., Jamal, J., Yang, W., Xian, M., Cai, T., Wen, E. Z., Jia, Q., Wang, P. G., and Poulos, T. L. (2002) The novel binding mode of N-alkyl-N′-hydroxyguanidine to neuronal nitric oxide synthase provides mechanistic insights into NO biosynthesis. *Biochemistry 41*, 13868−13875.
(37) Otwinowski, Z., and Minor, W. (1997) Processing of X-ray diffraction data collected in oscillation mode. *Methods Enzymol. 276*, 307−326.
(38) Murshudov, G. N., Vagin, A. A., and Dodson, E. J. (1997) Refinement of macromolecular structures by the maximum-likelihood method. *Acta Crystallogr. 53*, 240−255.
(39) Emsley, P., Lohkamp, B., and Scott, W. G. (2010) Features and development of Coot. *Acta Crystallogr. D66*, 486−501.
(40) Winn, M. D., Isupov, M. N., and Murshudov, G. N. (2001) Use of TLS parameters to model anisotropic displacements in macromolecular refinement. *Acta Crystallogr. D57*, 122−133.
(41) Martin, N. I., Woodward, J. J., and Marletta, M. A. (2006) NG-Hydroxyguanidines from primary amines. *Org. Lett. 8*, 4035−4038.
(42) Schade, D., Töpker-Lehmann, K., Kotthaus, J., and Clement, B. (2008) Synthetic approaches to N^{δ}-methylated L-arginine, N^{ω}-hydroxy-L-arginine, L-citrulline, and N^{δ}-cyano-L-ornithine. *J. Org. Chem. 73*, 1025−1030.
(43) van der Klei, I. J., Bystrykh, L. V., and Harder, W. (1990) Alcohol oxidase from *Hansenula polymorpha* CBS 4732. *Methods Enzymol. 188*, 420−427.
(44) Clague, M. J., Wishnok, J. S., and Marletta, M. A. (1997) Formation of N^{δ}-cyanoornithine from N^G-hydroxy-L-arginine and hydrogen peroxide by neuronal nitric oxide synthase: Implications for mechanism. *Biochemistry 36*, 14465−14473.
(45) Moali, C., Boucher, J.-L., Sari, M.-A., Stuehr, D. J., and Mansuy, D. (1998) Substrate specificity of NO synthases: Detailed comparison of L-arginine, homo-L-arginine, their Nω-hydroxy derivatives, and Nω-hydroxynor-L-arginine. *Biochemistry 37*, 10453−10460.
(46) Fast, W., Nikolic, D., van Breemen, R. B., and Silverman, R. B. (1999) Mechanistic studies of the inactivation of inducible nitric oxide synthase by N5-(1-Iminoethyl)-L-ornithine (L-NIO). *J. Am. Chem. Soc. 121*, 903−916.
(47) Brunel, A., Wilson, A., Henry, L., Dorlet, P., and Santolini, J. (2011) The proximal hydrogen bond network modulates *Bacillus subtilis* nitric-oxide synthase electronic and structural properties. *J. Biol. Chem. 286*, 11997−12005.